

Article

## Real-Time Fluorescence in Situ Visualization of Latent Fingerprints Exceeding Level 3 Details Based on Aggregation-Induced Emission

Ya-Long Wang, Chong Li, Hong-Qing Qu, Cheng Fan, Peng-Ju Zhao, Rui Tian, and Ming-Qiang Zhu

*J. Am. Chem. Soc.*, **Just Accepted Manuscript** • DOI: 10.1021/jacs.0c00124 • Publication Date (Web): 30 Mar 2020

Downloaded from [pubs.acs.org](https://pubs.acs.org) on April 4, 2020

### Just Accepted

“Just Accepted” manuscripts have been peer-reviewed and accepted for publication. They are posted online prior to technical editing, formatting for publication and author proofing. The American Chemical Society provides “Just Accepted” as a service to the research community to expedite the dissemination of scientific material as soon as possible after acceptance. “Just Accepted” manuscripts appear in full in PDF format accompanied by an HTML abstract. “Just Accepted” manuscripts have been fully peer reviewed, but should not be considered the official version of record. They are citable by the Digital Object Identifier (DOI®). “Just Accepted” is an optional service offered to authors. Therefore, the “Just Accepted” Web site may not include all articles that will be published in the journal. After a manuscript is technically edited and formatted, it will be removed from the “Just Accepted” Web site and published as an ASAP article. Note that technical editing may introduce minor changes to the manuscript text and/or graphics which could affect content, and all legal disclaimers and ethical guidelines that apply to the journal pertain. ACS cannot be held responsible for errors or consequences arising from the use of information contained in these “Just Accepted” manuscripts.

# Real-Time Fluorescence *in Situ* Visualization of Latent Fingerprints Exceeding Level 3 Details Based on Aggregation-Induced Emission

Ya-Long Wang<sup>‡</sup>, Chong Li<sup>‡,\*</sup>, Hong-Qing Qu, Cheng Fan, Peng-Ju Zhao, Rui Tian and Ming-Qiang Zhu\*

Wuhan National Laboratory for Optoelectronics, School of Optical and Electronic Information, College of Chemistry and Chemical Engineering, Huazhong University of Science and Technology, Wuhan, Hubei 430074, China.

**KEYWORDS** Latent fingerprints; aggregation-induced emission; fluorescence imaging; super-resolution imaging.

**ABSTRACT:** A water-soluble probe TPA-1OH with aggregation-induced emission (AIE) activity is synthesized and used for expedient real-time fluorescence *in situ* visualization of latent fingerprints (LFPs). TPA-1OH aqueous solution exhibits non-fluorescence in pure water while strong fluorescence upon molecular aggregating induced by addition of poor-solvent. Fluorescence images of LFPs on variety of substrates, including rough surfaces such as walls, bricks, paper, are developed under 405 nm light, by soaking in or spraying with TPA-1OH aqueous solution (30  $\mu$ M) without any necessity of organic co-solvents and post-treatment steps. The probe is non-cytotoxic at the concentration lower than 50  $\mu$ M. The development process of LFPs is demonstrated by real-time fluorescence *in situ* imaging. The exponential relationship between the relative fluorescence intensity and time is deduced from the fitting curve. The LFPs images developed by TPA-1OH are evident and intact enough to allow that the Level 1-3 details are displayed and analyzed. Noteworthy, the Level 3 details of LFPs such as the fingerprint ridge width, the characteristics of the sweat pores are evidently visible under fluorescence microscopy. Even the nanoscopic details exceeding Level 3 are visualized under super-resolution microscopy with sub-50 nm optical resolution.

## INTRODUCTION

Fingerprint is a unique characteristic of individual that remains unchanged throughout a person's life.<sup>1-3</sup> As an information feature that can serve as personal "ID cards" and "information banks", fingerprints are valuable evidences in criminal cases.<sup>2</sup> The latent fingerprints (LFPs) are formed due to the fingers touching, where are covered with sweat secreted by the sweat pores. Even the hand is thoroughly wiped and dried, if one person puts his hand on his face or hair, it is likely to leave LFPs on the place where he touches, especially objects with smooth surface such as metal, glass, ceramic and painted wood. LFPs are the most common type of fingerprint on crime scenes and hardly invisible by the naked eye. Hence, the development of LFPs is crucial for the detection of criminal cases.<sup>1-4</sup> At present, conventional LFPs development methods include powder dusting method, fuming method and chemical method.<sup>1</sup> However, these conventional methods suffer some limitations such as low contrast, sensitivity, selectivity, strong background interference and high toxicity.<sup>1</sup> The powder dusting method, which is currently the simplest and most commonly used method, is easy to damage the fingerprint details during the dusting process and the inevitable dust is harmful to the inspectors. The chemical reagents used in fuming and chemical methods, such as iodine, liquid cyanoacrylate esters, silver nitrate, ninhydrin and 1,8-diazafluoren-9-one (DFO) et al., can cause acute damage to the skin, eyes, mucous membranes or DNA.<sup>1</sup>

Subsequently, a variety of fluorescent materials, up-conversion nanoparticles (UCNP),<sup>5-7</sup> metal-organic frameworks,<sup>8</sup> quantum dots,<sup>9-14</sup> gold nanoparticles,<sup>15</sup> carbon dots<sup>16-18</sup> and semiconductor polymer dots,<sup>19</sup> have been reported

for LFPs development due to its higher contrast, higher selectivity, lower background interference compared to traditional methods.<sup>1-4</sup> However, these materials also suffer many shortcomings. For example, UCNPs and gold nanoparticles typically use rare earth metal and expensive metal materials, respectively. QDs usually contain toxic heavy metal ions such as Ge<sup>2+</sup>, Cu<sup>2+</sup>, and Mn<sup>4+</sup>.<sup>9-10, 14</sup> Besides, the solution methods based on quantum dots or carbon dots usually requires longer incubation time to ensure higher contrast (15 min to several hours).<sup>9, 14, 16</sup>

Since Tang discovered the aggregation-induced emission (AIE) phenomenon in 2001, AIE materials have been widely used in numerous fields due to their colorful fluorescence, easy functionalization, high contrast and intrinsic AIE characteristics.<sup>20,21</sup> In recent years, AIE nanoparticles and AIE powders were used to develop fingerprints in view of their rapid development, high contrast, high-resolution, and low toxicity (Table S1).<sup>22-31</sup> However, the popular AIE materials also suffer some limitations in practical applications. The disadvantages of AIE powders: 1) more consumption of materials; 2) may destroy the fingerprint details during the dusting process; 3) the dust may do harm to the health of the inspectors. The disadvantages of AIE nanoparticles: 1) commonly used binary solvent system CH<sub>3</sub>CN/H<sub>2</sub>O or EtOH/H<sub>2</sub>O, the organic solvent is easy to cause fingerprint damage;<sup>22-28</sup> 2) The preparation of the developer is troublesome because different substrates usually need different solvent ratios (Table S1); 3) Such nanoparticles are unstable and prone to aggregate, which is not conducive to long-term preservation; 4) customarily suitable for smooth substrates, usually glass, aluminum foils, stainless steel. Essentially, most of the fluorescent materials including current AIE materials suffer the essential problems: 1) The dyes are in

“on-on” mode, hence, the post-treatment after LFPs development, such as removing excess dye with water or air is indispensable to avoid interference of the residual dyes; 2) Except rare UCNP materials, most other dyes are irradiated under 365-nm light, which is unfriendly to the inspector; 3) The analysis for LFPs on Level 3 details are rarely reported due to the limitation of imaging mechanism; 4) The dyes with blue fluorescence display lower resolution and contrast, which are not conducive to the latent fingerprint detection in paper or plastic substrates which usually have inherent blue fluorescence.

To address the issues mentioned above, it is urgently desirable to develop the alternatives to conventional imaging probes of LFPs with the following characteristics: 1) simple-to-prepare and facile-to-operate to improve user experience; 2) nontoxic, water-soluble without any co-solvent and stabilizer, and activated by visible light to improve safety; 3) fluorescence “off-on” mode with long wavelength emission to improve contrast and resolution; 4) applicable for multi-substrates, even rough surface to improve the practicability. Here, we have designed and synthesized an AIE-based water-soluble probe TPA-1OH with red emission. The fluorescent probe shows remarkable capability on LFPs development with fluorescence “off-on” mode by immersing in or spraying with TPA-1OH aqueous solution without any organic co-solvents and additional post-treatment under 405 nm light. We have investigated the imaging mechanism, the screening of dye concentration and the corresponding cytotoxicity test. The development process of LFPs through *in situ* real-time imaging is demonstrated. Additionally, the development performance of LFPs on different substrates (such as tin foil, stainless steel, glass, leather, cardboard, wood, ceramic and plastic), even rough surfaces (such as walls, bricks, paper) is explored. The Level 3 details of LFPs such as the width of the fingerprint ridge and the characteristics of the sweat pores are analyzed. Noteworthy, even the nanoscopic pictures resolved by super-resolution imaging are visualized with sub-50 nm optical resolution, which is the very first report on LFPs.

## RESULTS AND DISCUSSION

**Synthesis and AIE Properties of TPA-1OH.** TPA-1OH was synthesized by the nucleophilic addition reaction of 4-

(diphenylamino)-benzaldehyde and compound 1 with a yield of 65% (Figure 1a). The detailed synthesis procedures of 4-(diphenylamino)-benzaldehyde, compound 1 and TPA-1OH were described in Supporting Information (SI). The target compound TPA-1OH was characterized by  $^1\text{H NMR}$ ,  $^{13}\text{C NMR}$ , LC-MS and HRMS. The UV-vis absorption spectrum of TPA-1OH in aqueous solution and the photoluminescence (PL) spectrum in the solid state were measured, respectively. The maximum absorption peak of TPA-1OH is located at 458 nm in water and the maximum emission peak is located at 660 nm in the solid state indicating its far-red fluorescence property (Figure 1b). The triphenylamine group is an excellent electron-donating group and serves as a hydrophobic end while the pyridyl cationic group has a strong electron-withdrawing effect and hydrophilicity. The lipid-water partition coefficient ( $P$ ) of TPA-1OH was measured as 1.40 in *n*-octanol/water system demonstrating that it is an amphiphilic compound, which is supported by the picture of TPA-1OH in *n*-octanol/water (Figure S1a and Table S2). It was observed that different concentrations of TPA-1OH was dissolved in water (5-50  $\mu\text{M}$ ) affording a clear solution (Figure S1b). The Beer-Lambert law experiment shows that the absorption intensity of TPA-1OH in water gradually increased with the increased concentration (Figure S1c), and the absorption value at 458 nm shows a linear relationship with the concentration (Figure S1d). It indicates that TPA-1OH can dissolve in water well within the test concentrations. TPA-1OH is soluble in water and high polar solvents such as THF, EtOH, MeOH, acetonitrile and water but insoluble in low polar solvents such as *n*-hexane, ether and ethyl acetate (EA). Therefore, the AIE property of TPA-1OH cannot be tested using common binary solvents such as THF/water or acetonitrile/water. Considered that water is slightly soluble in EA (wt. 2.94%), AIE property of TPA-1OH was tested in EA/water mixtures with EA fraction of 0 and 99%. No fluorescence was detected in aqueous solution while intense red fluorescence was measured in 99% ethyl acetate/water system with the peak at 652 nm (Figure 1c). The intense red fluorescence derives from the formation of nano-aggregated particles confirmed by Tyndall effect experiment and fluorescence microscopy imaging (Figure S2). The photoluminescence quantum yields (PLQY) of TPA-1OH were measured in aqueous solution and in the aggregate state as 0.058% and 7.5%, respectively (Table S3).

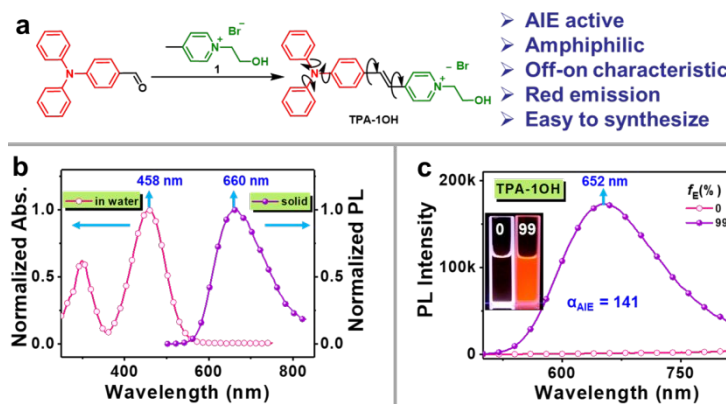


Figure 1. (a) The schematic synthesis of TPA-1OH. (b) Normalized absorption spectra and emission spectra of TPA-1OH in water (10  $\mu\text{M}$ ) and in solid state, respectively. (c) Emission spectra of TPA-1OH in water and in EA/water mixture with EA fraction of 99%. Inset: Fluorescence photographs of TPA-1OH in the EA/water mixtures with EA fraction of 0 and 99% under 365 nm irradiation (5  $\mu\text{M}$ ).

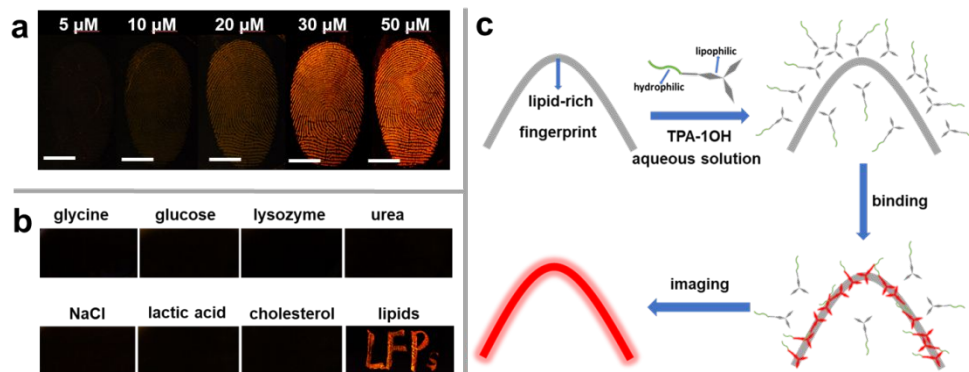


Figure 2. (a) The RGB true-color images of LFPs developed with aqueous solution of TPA-1OH with different concentrations under 405 nm irradiation (Scale bars: 5 mm). The corresponding grayscale images are shown in Figure S10. (b) Fluorescence photographs (under 405 nm irradiation) of characters “LFPs” written with different substances common in LFPs and sprayed with TPA-1OH aqueous solution. (c) The mechanism diagram of LFPs development using TPA-1OH aqueous solution.

**LFPs Development of TPA-1OH.** Fluorescence imaging is applied to LFPs development due to the high contrast and low background interference. AIE materials which overcome the inherent ACQ properties of traditional fluorescent materials have been reported on AIE molecules for LFPs development in recent years. LFPs development of AIE molecules is divided into the powder dusting method and solution method. Among them, the solution method is more studied due to its simple operation and low consumption of dyes. AIE compounds are typically prepared as nanoparticles in a binary system solution (usually acetonitrile/water or ethanol/water) as LFPs fluorescent development probes utilizing the lipophilicity of AIE molecular nanoparticles. However, the nanoparticles prepared by this binary system are unstable and prone to cause aggregation and precipitation, which cannot be stored for a long time. The solvent ratio of the binary system is various for different substrates, which is not beneficial for the standardization of procedure in practical application.<sup>22,23,26-28</sup> If LFPs could be developed by TPA-1OH, it would be a stable and easy-to-storage developer for LFPs due to water-soluble without any co-solvent and stabilizer, which provides much user-friendly experience. To evaluate the LFPs development effect of TPA-1OH, the foil paper with a fingerprint was immersed in aqueous solution of TPA-1OH at different concentration for 1 min. Under 405 nm irradiation, the fingerprint is gradually visible with the increase of dye concentration. The image of fingerprint is not evident at lower dye concentration (5  $\mu\text{M}$  and 10  $\mu\text{M}$ ) and clearly visible with the dye concentration at 30  $\mu\text{M}$  and 50  $\mu\text{M}$  (Figure 2a). The cytotoxicity of TPA-1OH was evaluated by MTT test which is closely related to the health of the inspector and has not seriously addressed in the reports for other LFPs fluorescent probes. The results shown that the dye exhibits nontoxicity at 0  $\mu\text{M}$ , 10  $\mu\text{M}$  and 30  $\mu\text{M}$  and low toxicity at 50  $\mu\text{M}$  (Figure S3). Therefore, the safe concentration of the dye is fixed at 30  $\mu\text{M}$  for LFPs development. The stability of TPA-1OH aqueous solution was checked by developing LFPs with fresh TPA-1OH (30  $\mu\text{M}$ ) aqueous solution and the one after stored for 3 months, respectively (Figure S4a). Nearly identical clear fingerprints were obtained by using above two developers and there were no significant differences in fluorescence signal contrast (Figure S4a inset). It indicates that the TPA-1OH aqueous solution can be stored for a long time (Figure S4a). Moreover, the

photostability of TPA-1OH in solid powder was measured upon continuous 405 nm irradiation for 10 min (Figure S4b). No obvious fluorescence decay was observed, suggesting an excellent photostability of TPA-1OH. In addition, the LFPs aged for 1 day, 3 days and 7 days on steel were developed with TPA-1OH aqueous solution. Clear images of fingerprints were obtained and there was nearly identical (Figure S4c). It means that aged LFPs have no significant effect on imaging results during a considerable time.

**LFPs Development mechanism of TPA-1OH.** To verify which component in LFPs can be recognized and combined with TPA-1OH, character “LFPs” pattern was written on the metal plate using the solution of main components in LFPs, such as glycine, glucose, lysozyme, urea, sodium chloride, lactic acid, cholesterol and lipids (mixture of lauric acid triglyceride and oleic acid), respectively. The dried character was drowned by an aqueous solution of TPA-1OH (30  $\mu\text{M}$ ). Under the 405 nm lamp, only the characters “LFPs” pattern written by the lipids component emitted strong fluorescence and was clearly visible, demonstrating that this probe did stain the lipid compounds in the LFPs (Figure 2b). The lipid-water partition coefficient (P) test results (Figure S1a and Table S2) show TPA-1OH has greater concentration in *n*-octanol than in  $\text{H}_2\text{O}$ , indicating the amphiphilic property with a preferred lipophilicity. The pyridine cation moiety, the hydrophilic end in the TPA-1OH structure, improves hydrophilicity, making the molecules soluble in water in a certain range of concentrations. When TPA-1OH aqueous solution is in contact with LFPs, the molecules will be adhered on lipid secretions in LFPs most probably due to the hydrophobic-hydrophobic interaction of lipid secretions phase in LFPs and lipophilic end of TPA-1OH. The mechanism is in consistency with those in the previous reports on development of LFPs with lipophilic AIE materials.<sup>22-24,27-31</sup> In addition, there may be electrostatic interaction between the positive charge of TPA-1OH and the natural negative charge of lipid secretions such as fatty acids, which also could contribute to the adhesion effect of TPA-1OH with lipid secretions.<sup>31</sup> In aqueous solution, TPA-1OH shows no fluorescence due to non-radiative transition. Once combined with lipid secretions in LFPs, TPA-1OH molecules are able to emit strong fluorescence due to restriction of intramolecular motion (RIM) induced by the viscosity effect of lipid secretions (Figure S5).

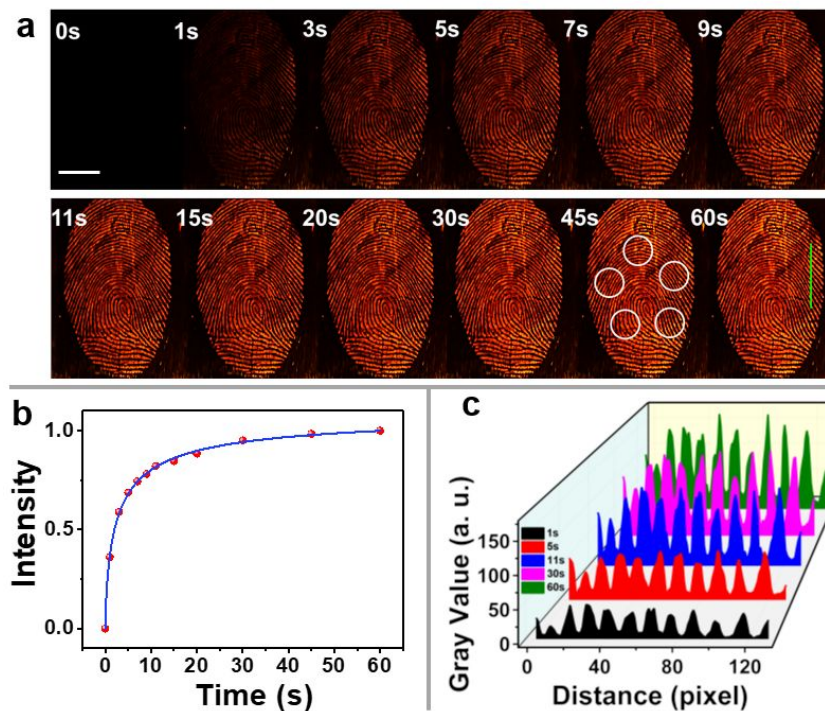


Figure 3. (a) Real-time fluorescence *in situ* development of LFPs on tinfoil in TPA-1OH aqueous solution under 405 nm irradiation (Scale bars: 5 mm). The corresponding grayscale images are shown in Figure S11. (b) The time-resolved changes of fluorescence intensity in the white circle regions. (c) The variations of fluorescence intensity contrast between the fingerprint ridges and furrow across the green line at different time.

**LFP Development Dynamics of TPA-1OH.** Compared to the previously reported “on-on” mode fluorescent probes, here the amphipathic dye TPA-1OH with “off-on” mode, which is not fluorescent in aqueous solution due to non-radiative transition, only shows strong fluorescence after being adhered on lipid secretions in the LFPs due to the RIM mechanism. Hence, the visualization process of LFPs development can be presented by real-time fluorescence *in situ* imaging experiments with the aid of this amphipathic “off-on” LFPs probe. As shown in Figure 3a, the profile of the fingerprint became gradually visible after 3 s and the vein of the fingerprint was gradually legible. Finally, the clear fingerprint pattern was observed in about 11 s, indicating the expedient *in situ* imaging ability of TPA-1OH (Figure 3a and Video S1). Next, the change of fluorescence intensity in the white circle regions at different time was analyzed. As shown in Figure 3b, the fluorescence intensity increased rapidly to almost the half maximum in the first 5 s and then increased slowly. After 30 s, the fluorescence intensity hardly changed, which is consistent with the images in Figure 3a. The staining dynamics of TPA-1OH with LFPs is based on the fitting of experimental data to a mathematical model as

$$I = 1 - e^{-kt} \quad \text{or} \\ \ln[1/(1-I)] = kt$$

where  $I$  is the normalized fluorescence intensity upon staining at time ( $t$ ), and  $k$  is the rate constant, which is calculated to be 0.48. The exponential relationship between the relative fluorescence intensity and time is deduced from the fitting curve, which is transformed into a linear curve (Figure S6).

The variation of signal intensity between the fingerprint ridges and furrows across the green line was also monitored.

The fingerprint ridges contain lipid secretions that are easily stained by TPA-1OH to show fluorescent signals, while the furrow shows no signals due to no sweat secretions. The contrast between fingerprint ridges and furrows was gradually increased with time, and a high contrast was obtained at 11 s. Combining with the changes of fluorescence intensity and contrast, the fingerprint images with clear ridges and high contrast across the green line could be real-time developed by TPA-1OH, indicating a rapid development capacity (Figure 3c).

#### Substrate Generality of TPA-1OH for LFPs Development.

To study the universality of TPA-1OH probe, the LFPs developments on different substrates were conducted by dipping in TPA-1OH (30  $\mu\text{M}$  in water) for 1 min, such as tinfoil, stainless steel, glass, leather, cardboard, wood, ceramic and plastic. It was observed that the LFPs on different substrates were developed successfully, affording the clear fingerprint pictures with high contrast and high-resolution (Figure 4a). Compared with other substrates, the paper card was stained with a red background probably due to the penetration of TPA-1OH aqueous solution, but the fingerprint pattern is still clear due to the strong fluorescence contrast. Substrate, environment, and fingerprint composition are identified as the main primary influences on the successful detection of LFPs.<sup>32</sup> There is no essential difference in fingerprint collection methods. The substrate is often the priority consideration for choosing a visualization technique. The imaging result is mainly related to the quality of LFPs themselves on examining substrates.<sup>32</sup> Comparing the LFPs images recorded by soaking the samples in (Figure 3a) and the ones by taking the samples out (Figure 4 and Figure S4) from the TPA-1OH aqueous solution, the resolution of the images is

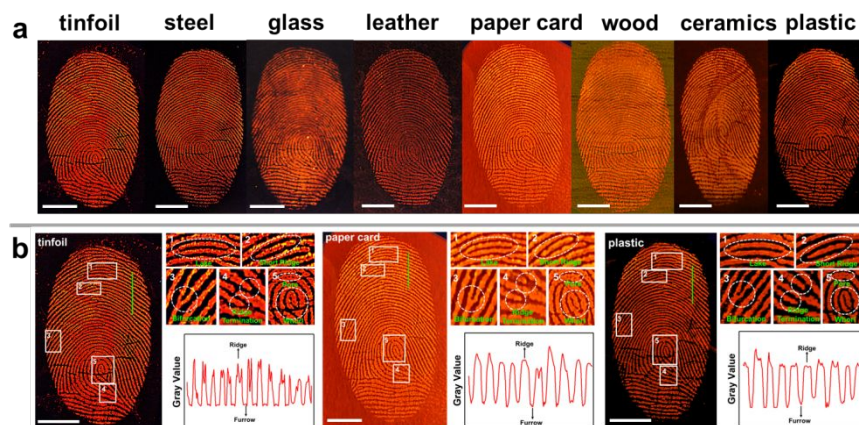


Figure 4. (a) RGB true-color photographs (under 405 nm irradiation) of whole LFPs on different substrates developed by TPA-1OH aqueous solution (Scale bars: 5 mm). (b) Level 1, Level 2 and Level 3 details of local LFPs on the foil, paper card and plastic developed by TPA-1OH aqueous solution and the variations of the fluorescence intensity between the fingerprint ridges and furrows across the green line (Scale bars: 5 mm). Level 1: refer to the overall characteristics of the whole fingerprint, including the shape of the fingerprint (whorl, loop, arch, etc.), the core point (or called the center point) and the triangle point. Level 2 details are the macroscopic detail feature of the fingerprint ridge, generally dividing into ending, bifurcation, island, and short ridge. Level 3 details are the microscopic detail feature of the fingerprint, which mainly includes the shape of the ridge edge, the width of the ridge and pore. The corresponding grayscale images are shown in Figure S12.

not significantly changed, and clear fingerprint patterns can be obtained, indicating the treatment of drying process has no noticeable influence on imaging quality of the developed LFPs. Usually, fingerprints are analyzed by three levels of detail to identify individual identity. Level 1, which are not unique enough to identify individual identity, refer to the overall characteristics of the fingerprint, including the shape of the fingerprint, the core point (or called the center point) and the triangle points. The shapes of the fingerprint at Level 1 are divided into whorl, loop, arch, etc. Level 2 details are the macroscopic detail feature of the fingerprint ridge, generally dividing into ending, bifurcation, island, and short ridge. Level 3 details are the microscopic detail feature of the fingerprint, which mainly includes the shape of the ridge edge, the width of the ridges and pores. Level 2 and Level 3 details are often used to recognize the individual identity due to the unique feature. To verify the fingerprints detail, Level 1, Level 2 and Level 3 details of the fingerprints on the foil, paper card and plastic are analyzed. In the magnified images, whorl (Level 1), lake, short ridge, bifurcation and ridge termination (Level 2), and pore (Level 3) are clearly visible by naked eye, which can provide reliable evidence for the reorganization of individual identity (Figure 4b). Besides, the fluctuation of the fluorescence intensity between the fingerprint ridges and furrows across the green line shows the high contrast between the fingerprint ridges and substrate. It is worth mentioning that these LFPs details were obtained without any post-treatment such as heating or chemical post-treatment, but simply dipping in or spraying with TPA-1OH aqueous solution (Figure S7 and Video S2). Both the soaking method and spraying method are extremely practical methods with their own advantages. The soaking method without post-treatment is easy-to-operate at the scenes and seems more suitable for water-resist materials (tinfoil, steel, glass, plastic, etc.) with high resolution due to the thoroughly and uniformly covering of the dye solution. The spraying method is not restricted by the substrate materials, and shows numerous merits, such as facile, fast, highly sensitive, economic and large-area operable, which is the most promising

method for LFPs development in practical applications. In general, these two development methods are safe, clean, easy-to-store, economic, simple-to-operate and high-efficient, which are both convenient and practical for LFPs development in different scenarios.

Furthermore, the rubbings of LFPs images on the different substrates were collected by forensic fingerprint tape. The rubbings of LFPs images remained clear and intact although the fluorescent color of the rubbings became yellow probably because the glue of the fingerprint tape affected the fluorescent color. The detail feature of the LFPs images and the rubbings of LFPs images on tinfoil and plastic are analyzed and compared (Figure S8). In the magnified images, whorl (Level 1), lake, short ridge, bifurcation and ridge termination (Level 2), and pore (Level 3) are clearly visible by naked eye, indicating that the fingerprint can be collected by forensic fingerprint tape. This is beneficial for the acquisition of latent fingerprints on curving substrates, such as cup, steel tube, bottle, etc. because the entire fingerprint on curving substrates is difficult to be focused by the camera, causing the failure to capture clear and complete fingerprint images. Overall, through the safe and simple TPA-1OH aqueous solution method, LFPs with high contrast and high-resolution details are developed on different substrates including rough surfaces such as wall, brick, paper, which validates the high practicability of this system for individual identification.

#### TPA-1OH for LFPs Development Down to Level 3 Details.

Incomplete fingerprints with only Level 1 and Level 2 details are usually accessible at the crime scene. It is much difficult in forensic science to identify and authenticate individuals based on only the Level 1 and Level 2 details of fingerprints. At this point, the Level 3 microscopic details of the fingerprint, such as the edge shape of the ridges, the width and narrowness of the ridges, and the characteristics of sweat pores become particularly important. The Level 3 microscopic details of fingerprints from volunteers were explored by a fluorescence microscope

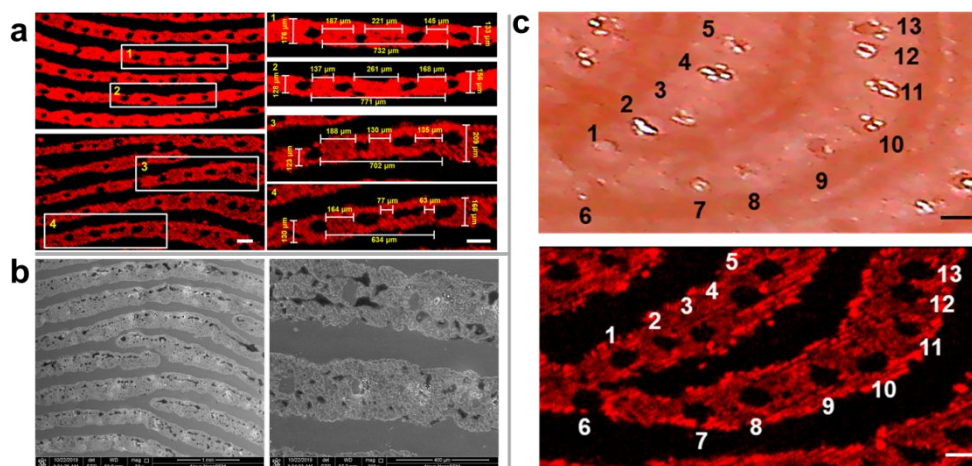


Figure 5. (a) Fluorescence microscopic images for partial region of the latent fingerprints from volunteers and the analysis of Level 3 microscopic details. Compared with the images in Figure 4, the cores and shape of the ridges are visualized with definite sizes. The sweat cores (Diameter 80-120 nm) are identified to be aligned periodically in each 100-200 nm along with the ridges. (b) The SEM images of fingerprint. (c) The number and location distribution of sweat pores on the bifurcation of the real fingerprint (top) on finger and its developed fingerprint (bottom) on substrate from volunteer. The fluorescent pattern of LFP is much more decipherable than other type ones (Scale bars: 100  $\mu\text{m}$ ).

(Figure 5a left). The number, location and distribution of sweat pores in two-dimension space on the fingerprint patterns can be evidently observed. The distances between different sweat pores on the same ridge are different. Besides, the widths of the different ridges and even different positions of sweat pores on the same ridge could be distinguished (Figure 5a right). The fingerprint ridges in similar scale could be also observed by SEM (Figure 5b). Actually, the fluorescence images exhibit higher contrast than SEM. We can clearly observe the distribution of sweat holes in fluorescence images while the poor contrasts of SEM images are obtained. These unique characteristics of the information can provide valid and reliable evidence for individual identification. Moreover, real

fingerprint bright field image and developed fingerprint fluorescence image of the same area from volunteer were collected, respectively. By comparing the number, location and distribution of sweat pores on the bifurcation, the developed fingerprint fluorescence image is highly matched with the real fingerprint on the finger (Figure 5c), indicating that the probe TPA-1OH excels in individual identification and authentication from fingerprint on Level 3 details.

**TPA-1OH for LFPs Super-Resolution Imaging.** To obtain more detailed information of LFPs exceeding Level 3, super-resolution fluorescent imaging is employed to acquire the nanoscopic details of LFPs. The partial region LFPs could be

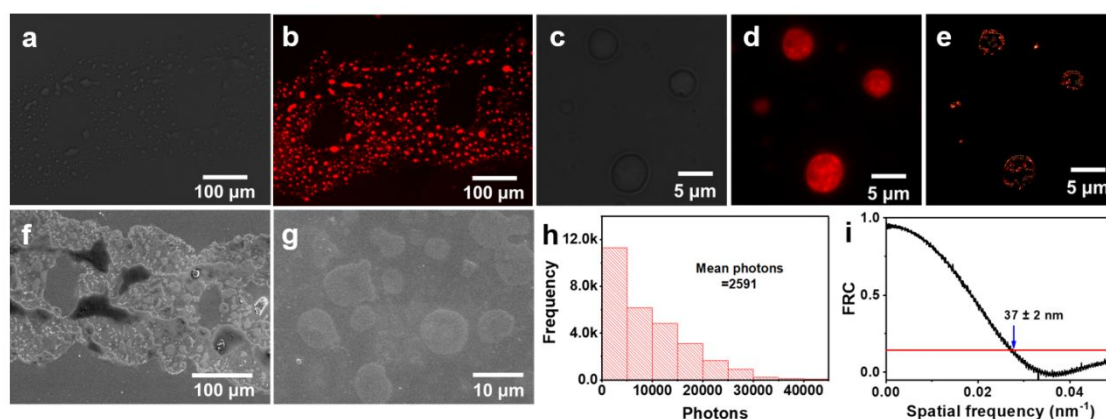


Figure 6. The micro-morphology of LFPs characterized by optical imaging and SEM. (a) Bright field image and (b) conventional fluorescence image of partial region of the LFPs ridges from one volunteer (objective: 10 $\times$ ). (c) Bright field image, (d) conventional fluorescent image and (e) super-resolution image of the lipid deposit spots at the same region in a LFPs ridge with larger magnification than that of (a) (objective: 100 $\times$ ). SEM images of the LFPs ridge at the magnification of (f) 600 $\times$  and (g) 5000 $\times$ , respectively. (h) The photon count distribution at each localization event in super-resolution imaging of (e). The mean number of photons was calculated using a single-exponential fit. (i) The overall resolution of (e) determined by Fourier ring correlation (FRC). The LFPs samples for the optical imaging are soaked in TPA-1OH aqueous solution. The LFPs samples for SEM are pre-soaked with water to remove the water-soluble secretions and then dried at room time before test.

roughly recognized in the bright field optical image (Figure 6a). The clear outline of LFPs and sweat pores could be observed in the conventional fluorescence image after staining of TPA-1OH (Figure 6b). It is observed that the fingerprints are composed with plenty of deposits in different sizes which is consistent with the SEM images (Figure 6f and 6g). It is reported that the main component of these deposits in different sizes is lipid secreted by human body.<sup>33</sup> Hence, the spots are mainly lipid deposits, which are tiny constituent units of LFPs ridges (Figure 6c). Fluorescence imaging integrating with super-resolution imaging could intuitively observe lipid deposits with higher resolution and help deepen understanding of lipid deposits. The micron-sized spots in Figure 6d is the conventional fluorescence image of lipid deposits spots stained with TPA-1OH in Figure 6c. Considering the limit resolution of conventional optical imaging, we attempted to explore the finer structure of the deposit spots with higher resolution methods. Figure 6e is the super-resolution image of the same deposit spots of figure 6c and 6d. The overall resolution of a diffraction-unlimited image determined by Fourier ring correlation (FRC) is counted to  $37 \pm 2$  nm (Figure 6i). The mean number of photons at each localization even in super resolution imaging was 2500, exhibiting the super-resolution imaging capability of TPA-1OH. As expected, the size and distribution of lipid deposit spots characterized by super-resolution imaging are similar with those of SEM (Figure 6g). The super-resolution image shows a clearer outline and finer nanostructure of lipid deposits than those of the conventional one although the characteristic nanostructures are not obtained. Super-resolution imaging is of great significance for deeper understanding the micro-structure of LFPs by stained with TPA-1OH. It indicates that TPA-1OH molecules are indeed adhered on lipid secretions in LFPs driven mainly by the hydrophobic-hydrophobic interactions between the lipid secretions in LFPs and the hydrophobic part of TPA-1OH molecules.

The development of LFPs is an important focusing subject of forensic science due to its uniqueness in public security. At present, many methods of fingerprint development have been extensively utilized. However, these methods often suffer some limitations. On one hand, the traditional methods are utilized mostly in rough level due to the limitations of low contrast, low resolution and high toxicity. On the other hand, the reported fluorescent development probes of LFPs almost all need post-treatment after fingerprint development due to the “on-on” mode and are irradiated under UV light (such as 365-nm). In addition, the development of LFPs on Level 3 details are rarely reported. Here, we reported a new water-soluble probe TPA-1OH with AIE-activity which shows remarkable capability on LFPs development with fluorescence “off-on” mode by immersing in or spraying with TPA-1OH aqueous solution under visible light irradiation (such as 405 nm). Compared with previous reports, here the probe TPA-1OH exhibits the excellent potentials as follow: 1) easy to synthesize in large scale only by simple 3-steps reactions; 2) safer due to nontoxic, visible light excitation and aqueous solution in 100% water without any organic co-solvents and stabilizer; 3) facile to perform by simply immersing the evidence in or spraying the evidence surface with TPA-1OH aqueous solution without any other post-treatment; 4) extensively applicable for multi-substrates, even rough surfaces, such as walls, bricks, paper; 5) high contrast and high resolution of LFPs images owing to the “off-on” characteristic and red emission of the probe; 6) the unprecedented nanoscopic details of LFPs acquired by super-

resolution microscopy. Apparently, these features are beneficial for LFPs collection in crime scenes. In the process of *on-site* fingerprint collection in forensic science, user experience and fingerprint fidelity are the primary considerations. Therefore, we believe that the probe can excel perfectly in the *on-site* fingerprint acquisition program, providing an alternative solution for the development of standardized procedure of reliable fingerprints collection in forensic science.

## CONCLUSION

In conclusion, an AIE-based red fluorescent LFPs probe TPA-1OH is synthesized with hydrophilic-hydrophobic molecular architecture. The probe aqueous solution shows no fluorescence due to non-radiative energy transfer while strong red fluorescence is developed due to restriction of intramolecular motion (RIM) upon the hydrophobic end adhered on the lipid secretion of the fingerprint. Thanks to the “off-on” characteristic of TPA-1OH, real-time fluorescence *in situ* visualization of LFPs was successfully implemented. The fingerprint contours could be observed in a few seconds. The legible fingerprint pattern with high contrast and resolution could be observed in 30 s. Moreover, the visualization images of LFPs can be collected completely by forensic fingerprint tape, which is beneficial for fingerprints acquisition on curving substrates. Both the visualization images and the rubbings of LFPs images could provide Level 1-3 details of the fingerprint, which can provide reliable evidence for the reorganization of individual identity. The Level 3 details of LFPs such as the width of the fingerprint ridge and the characteristics of the sweat pores can be observed in fluorescence microscope. For incomplete LFPs, individual identity can be determined by analysis of Level 3 details such as the number and location distribution of sweat pores in two dimension and the width of fingerprint ridges. It is unprecedented that the nanoscopic details of LFPs could be acquired by super-resolution microscopy. In addition, it can be promising as an indicator for some fuzzy and illegible fingerprints to facilitate forensic extraction of the suspects DNA information. It can be expected that this probe will effectively develop LFPs at the scene of the crime in near future.

## ASSOCIATED CONTENT

**Supporting Information.** Materials and methods. This material is available free of charge via the Internet at <http://pubs.acs.org>.

## AUTHOR INFORMATION

### Corresponding Author

\* mqzhu@hust.edu.cn; chongli@hust.edu.cn

### Author Contributions

‡ These authors contributed equally.

## ACKNOWLEDGMENT

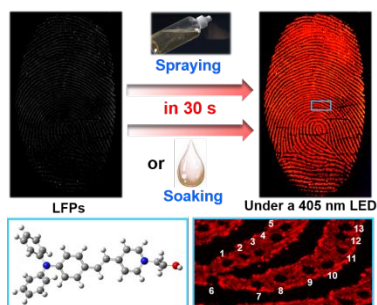
This work was supported by the National Basic Research Program (973) of China (2015CB755602 and 2013CB922104), the National Natural Science Foundation of China (51673077, 21474034 and 51603078), the Fundamental Research Funds for the Central Universities (HUST: 2019kfyXKJC035 and HUST: 2018KFYXKJC033), and the Natural Science Foundation of Hubei Province (2018CFB574). We also thank Analytical and Testing Center of Huazhong University of Science and Technology and the

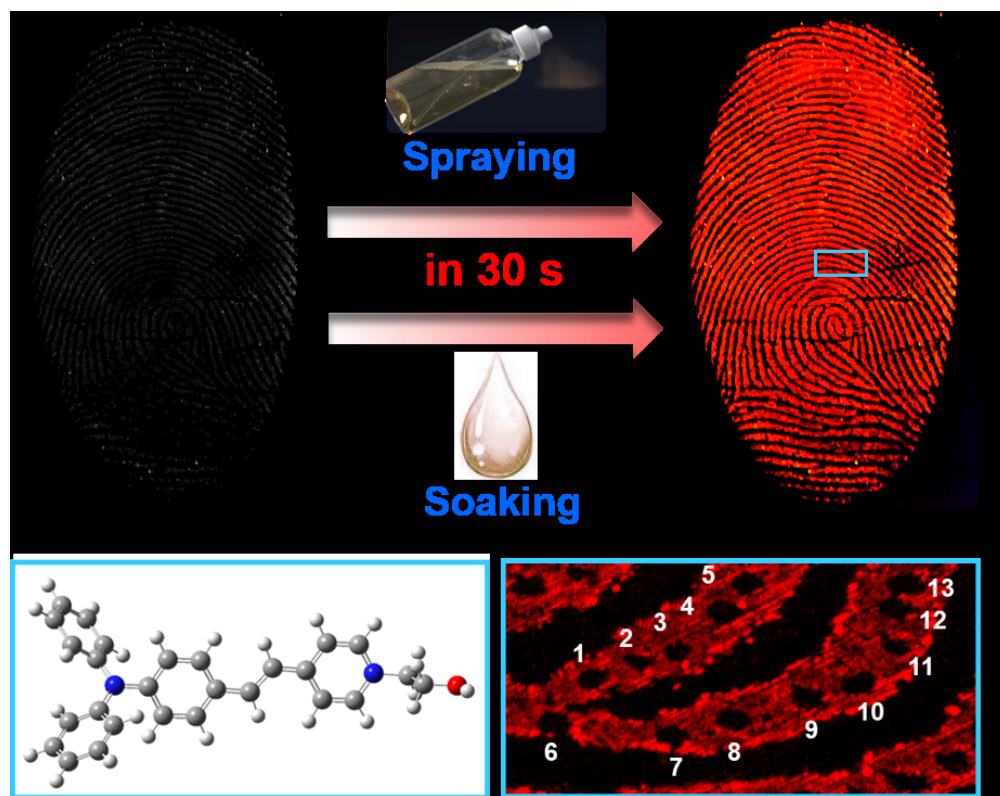
Center of Micro-Fabrication and Characterization (CMFC) of WNLO for use of their facilities.

## REFERENCES

1. Wang, M.; Li, M.; Yu, A.; Zhu, Y.; Yang, M.; Mao, C., Fluorescent Nanomaterials for the Development of Latent Fingerprints in Forensic Sciences. *Adv. Funct. Mater.* **2017**, *27*, 1606243.
2. Wang, Y.; Wang, J.; Ma, Q.; Li, Z.; Yuan, Q., Recent progress in background-free latent fingerprint imaging. *Nano Res.* **2018**, *11*, 5499.
3. Wei, Q.; Zhang, M.; Ogorevc, B.; Zhang, X., Recent advances in the chemical imaging of human fingermarks. *Analyst* **2016**, *141*, 6172.
4. Becue, A., Emerging fields in fingermark (meta) detection—a critical review. *Anal. Methods* **2016**, *8*, 7983.
5. Wang, M.; Li, M.; Yang, M.; Zhang, X.; Yu, A.; Zhu, Y.; Qiu, P.; Mao, C., NIR-induced highly sensitive detection of latent fingermarks by NaYF<sub>4</sub>:Yb, Er upconversion nanoparticles in a dry powder state. *Nano Res.* **2015**, *8*, 1800.
6. Ma, R.; Bullock, E.; Maynard, P.; Reedy, B.; Shimmon, R.; Lennard, C.; Roux, C.; McDonagh, A., Fingermark detection on non-porous and semi-porous surfaces using NaYF<sub>4</sub>:Er,Yb up-converter particles. *Forensic Sci. Inter.* **2011**, *207*, 145.
7. Ma, R.; Shimmon, R.; McDonagh, A.; Maynard, P.; Lennard, C.; Roux, C., Fingermark detection on non-porous and semi-porous surfaces using YVO<sub>4</sub>:Er,Yb luminescent upconverting particles. *Forensic Sci. Inter.* **2012**, *217*, E23.
8. Wang, M.; Guo, L.; Cao, D., Metal-organic framework as luminescence turn-on sensor for selective detection of metal ions: Absorbance caused enhancement mechanism. *Sensors Actuat. B-Chem.* **2018**, *256*, 839.
9. Li, Z.; Wang, Q.; Wang, Y.; Ma, Q.; Wang, J.; Li, Z.; Li, Y.; Lv, X.; Wei, W.; Chen, L.; Yuan, Q., Background-free latent fingerprint imaging based on nanocrystals with long-lived luminescence and pH-guided recognition. *Nano Res.* **2018**, *11*, 6167.
10. Raju, G. S. R.; Park, J. Y.; Nagaraju, G. P.; Pavitra, E.; Yang, H. K.; Moon, B. K.; Yu, J. S.; Huh, Y. S.; Jeong, J. H., Evolution of CaGd<sub>2</sub>ZnO<sub>5</sub>:Eu<sup>3+</sup> nanostructures for rapid visualization of latent fingerprints. *J. Mater. Chem. C* **2017**, *5*, 4246.
11. Shi, Y.; Ye, J.; Qi, Y.; Akram, M. A.; Rauf, A.; Ning, G., An anionic layered europium(III) coordination polymer for solvent-dependent selective luminescence sensing of Fe<sup>3+</sup> and Cu<sup>2+</sup> ions and latent fingerprint detection. *Dalton Trans.* **2018**, *47*, 17479.
12. Sandhyarani, A.; Kokila, M. K.; Darshan, G. P.; Basavaraj, R. B.; Prasad, B. D.; Sharma, S. C.; Lakshmi, T. K. S.; Nagabhushana, H., Versatile core-shell SiO<sub>2</sub>@SrTiO<sub>3</sub>:Eu<sup>3+</sup>, Li<sup>+</sup> nanopowders as fluorescent label for the visualization of latent fingerprints and anti-counterfeiting applications. *Chem. Eng. J.* **2017**, *327*, 1135.
13. Marappa, B.; Rudresha, M. S.; Basavaraj, R. B.; Darshan, G. P.; Prasad, B. D.; Sharma, S. C.; Sivakumari, S.; Amudha, P.; Nagabhushana, H., EGCG assisted Y<sub>2</sub>O<sub>3</sub>:Eu<sup>3+</sup> nanopowders with 3D micro-architecture assemblies useful for latent fingerprint recognition and anti-counterfeiting applications. *Sensors Actuat. B-Chem.* **2018**, *264*, 426.
14. Wang, J.; Ma, Q.; Liu, H.; Wang, Y.; Shen, H.; Hu, X.; Ma, C.; Yuan, Q.; Tan, W., Time-Gated Imaging of Latent Fingerprints and Specific Visualization of Protein Secretions via Molecular Recognition. *Anal. Chem.* **2017**, *89*, 12764.
15. Cheng, Y.-H.; Zhang, Y.; Chau, S.-L.; Lai, S. K.-M.; Tang, H.-W.; Ng, K.-M., Enhancement of Image Contrast, Stability, and SALDI-MS Detection Sensitivity for Latent Fingerprint Analysis by Tuning the Composition of Silver-Gold Nanoalloys. *ACS Appl. Mater. Inter.* **2016**, *8*, 29668.
16. Chen, J.; Wei, J.-S.; Zhang, P.; Niu, X.-Q.; Zhao, W.; Zhu, Z.-Y.; Ding, H.; Xiong, H.-M., Red-Emissive Carbon Dots for Fingerprints Detection by Spray Method: Coffee Ring Effect and Unquenched Fluorescence in Drying Process. *ACS Appl. Mater. Inter.* **2017**, *9*, 18429.
17. Wang, C.-F.; Cheng, R.; Ji, W.-Q.; Ma, K.; Ling, L.; Chen, S., Recognition of Latent Fingerprints and Ink-Free Printing Derived from Interfacial Segregation of Carbon Dots. *ACS Appl. Mater. Inter.* **2018**, *10*, 39205.
18. Fernandes, D.; Krysmann, M. J.; Kelarakis, A., Carbon dot based nanopowders and their application for fingerprint recovery. *Chem. Commun.* **2015**, *51*, 4902.
19. Cui, J.; Xu, S.; Guo, C.; Jiang, R.; James, T. D.; Wang, L., Highly Efficient Photothermal Semiconductor Nanocomposites for Photothermal Imaging of Latent Fingerprints. *Anal. Chem.* **2015**, *87*, 11592.
20. Mei, J.; Leung, N. L. C.; Kwok, R. T. K.; Lam, J. W. Y.; Tang, B. Z., Aggregation-Induced Emission: Together We Shine, United We Soar! *Chem. Rev.* **2015**, *115*, 11718.
21. Wang, Y.-F.; Zhang, T.; Liang, X.-J., Aggregation-Induced Emission: Lighting up Cells, Revealing Life! *Small* **2016**, *12*, 6451.
22. Xu, L.; Li, Y.; Li, S.; Hu, R.; Qin, A.; Tang, B. Z.; Su, B., Enhancing the visualization of latent fingerprints by aggregation induced emission of siloles. *Analyst* **2014**, *139*, 2332.
23. Li, Y.; Xu, L.; Su, B., Aggregation induced emission for the recognition of latent fingerprints. *Chem. Commun.* **2012**, *48*, 4109.
24. Singh, P.; Singh, H.; Sharma, R.; Bhargava, G.; Kumar, S., Diphenylpyrimidinone-salicylideneamine - new ESIPT based AIEgens with applications in latent fingerprinting. *J. Mater. Chem. C* **2016**, *4*, 11180.
25. Singh, H.; Sharma, R.; Bhargava, G.; Kumar, S.; Singh, P., AIE plus ESIPT based red fluorescent aggregates for visualization of latent fingerprints. *New J. Chem.* **2018**, *42*, 12900.
26. Jin, X.; Dong, L.; Di, X.; Huang, H.; Liu, J.; Sun, X.; Zhang, X.; Zhu, H., NIR luminescence for the detection of latent fingerprints based on ESIPT and AIE processes. *RSC Adv.* **2015**, *5*, 87306.
27. Jin, X.; Xin, R.; Wang, S.; Yin, W.; Xu, T.; Jiang, Y.; Ji, X.; Chen, L.; Liu, J., A tetraphenylethene-based dye for latent fingerprint analysis. *Sensors Actuat. B-Chem.* **2017**, *244*, 777.
28. Suresh, R.; Thiyagarajan, S. K.; Ramamurthy, P., An AIE based fluorescent probe for digital lifting of latent fingerprint marks down to minutiae level. *Sensors Actuat. B-Chem.* **2018**, *258*, 184.
29. Zhang, S.; Liu, R.; Cui, Q.; Yang, Y.; Cao, Q.; Xu, W.; Li, L., Ultrabright Fluorescent Silica Nanoparticles Embedded with Conjugated Oligomers and Their Application in Latent Fingerprint Detection. *ACS Appl. Mater. Inter.* **2017**, *9*, 44134.
30. Wang, M.; Guo, L.; Cao, D., Covalent Organic Polymers for Rapid Fluorescence Imaging of Latent Fingerprints. *ACS Appl. Mater. Inter.* **2018**, *10*, 21619.
31. Malik, A. H.; Kalita, A.; Iyer, P. K., Development of Well-Preserved, Substrate-Versatile Latent Fingerprints by Aggregation-Induced Enhanced Emission-Active Conjugated Polyelectrolyte. *ACS Appl. Mater. Inter.* **2017**, *9*, 37501.
32. Kanodarwala, F. K.; Moret, S.; Spindler, X.; Lennard, C.; Roux, C., Nanoparticles used for fingermark detection—A comprehensive review. *Forensic Sci.* **2019**, *1*, 1341.
33. Dorakumbura, B. N.; Boseley, R. E.; Becker, T.; Martin, D. E.; Richter, A.; Tobin, M. J.; van Bronswijk, W.; Vongsvivut, J.; Hackett, M. J.; Lewis, S. W., Revealing the spatial distribution of chemical species within latent fingermarks using vibrational spectroscopy. *Analyst* **2018**, *143*, 4027.

## SYNOPSIS TOC (Word Style "SN\_Synopsis\_TOC").





32 A water-soluble AIE probe is developed for real time fluorescence in situ visualization of latent fingerprints  
33 exceeding Level 3 details on a variety of substrates.

34 156x123mm (150 x 150 DPI)